# Dioxygen and Hydrogen Peroxide Reduction with Hemocyanin Model Complexes

Matthew A. Thorseth, Christopher S. Letko, Thomas B. Rauchfuss, and Andrew A. Gewirth*

Department of Chemistry, University of Illinois at Urbana—Champaign, 600 S. Mathews Avenue, Urbana, Illinois 61801, United States

S *Supporting Information*

ABSTRACT: Three copper polypyridyl complexes were examined as electrocatalysts for the oxygen reduction reaction (ORR): a Cu−N$_3$ complex, [Cu−[tris(6-methylpyridin-2-yl)methane]-(NCMe)]PF$_6$ (**1**); a related Cu$_2$N$_6$ derivative, [Cu$_2$−[1,2-bis(6-(bis(6-methyl-pyridin-2-yl)methyl)pyridin-2-yl)ethane]-(NCMe)$_2$](PF$_6$)$_2$ (**2**); and the CuN$_4$ species [Cu−[tris(pyridin-2-ylmethyl)amine]](ClO$_4$)$_2$ [**3**](ClO$_4$)$_2$. Compared to other copper complexes, [**3**](ClO$_4$)$_2$ exhibits the highest reported ORR onset potential for a Cu complex of 0.53 V vs reversible hydrogen electrode at pH 1. The Cu$_2$N$_6$ hemocyanin model is more active than the CuN$_3$, but both are less active than the CuN$_4$ complex. The results indicate that copper polypyridyl complexes are promising cathode catalysts for ORR.
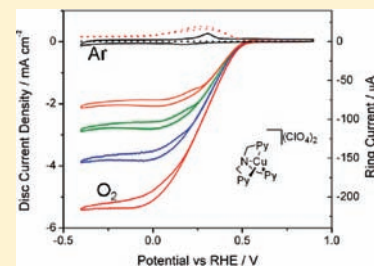
■ INTRODUCTION

One of the greatest hurdles to the widespread implementation of fuel cells is the cathode catalyst.[1,2] In most fuel cells, the cathode catalyzes the 4e⁻ reduction of dioxygen to water (eq 1).

$$O_2 + 4e^- + 4H^+ \rightarrow 2H_2O \qquad E = 1.17 \text{ V at pH 1} \quad (1)$$

Current fuel cells rely on Pt-based cathodes, which exhibit slow reaction kinetics for the oxygen reduction reaction (ORR).[3,4] To mitigate the slow kinetics for the ORR, high catalyst loadings are required, which translate into high cost. Additionally, Pt-based ORR catalysts evince a ca. 300 mV overpotential for the ORR, which seriously diminishes fuel cell efficiency. Although the performance of Pt-based catalysts has been improved by alloying and developments in catalyst morphology, substantial improvement in catalyst composition is required,[5] and ultimately Pt may be replaced by base metals.

One source of inspiration for a new class of ORR catalysts comes from nature in the form of laccase, an enzyme that exhibits a lower overpotential for the ORR compared to Pt.[6] The active site of laccase is composed of three Cu atoms, two that are coordinated by three histidine groups, known as the type-3 copper centers, and one that is ligated by two histidine groups, known as the type-2 copper.[7−9] When considering new generations of bioinspired cathode catalysts, it is noteworthy that type-3 copper centers are observed in a large variety of enzymes that activate O$_2$, such as tyrosinase (Tyr) and hemocyanin (Hc).[10] Tyrosinase catalyzes the oxidation of phenols and catechols coupled with the reduction of oxygen to water, and hemocyanin is a reversible dioxygen carrier.[9,11,12] The dioxygen adducts of Hc and Tyr both feature bridging peroxo ligands with a $\mu-\eta^2{:}\eta^2$ diamondoid motif. The differing reactivity of Tyr and Hc is due to the ability of phenols and catechols to access the active site in tyrosinase, but not in hemocyanin.[9]
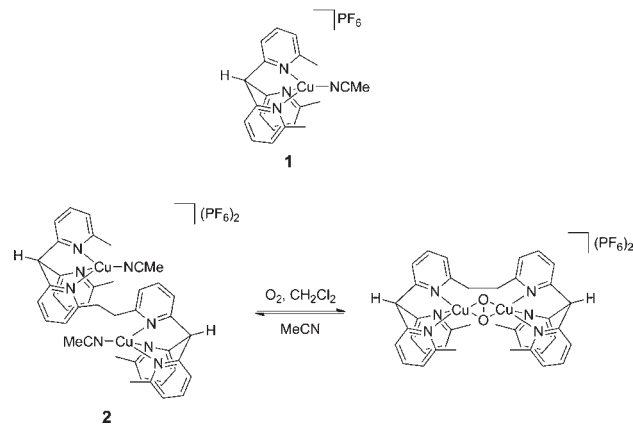

Figure 1. Hemocyanin models [Cu(tripic)(NCMe)]PF$_6$ (**1**) and [Cu$_2$(bistripic)(NCMe)$_2$](PF$_6$)$_2$ (**2**), which reversibly oxygenates.

An excellent synthetic model for Hc is Kodera's hexapicolinyl dicopper complex, which reversibly forms a $\mu-\eta^2{:}\eta^2$ dioxygen complex that is stable for hours at room temperature (Figure 1).[13−15] Although many Cu complexes have been described as spectroscopic and structural models for hemocyanin, none appear to have been tested for their activity in the ORR. In previous work we and others have demonstrated that other synthetic Cu-based complexes catalyze ORR over a wide range of pHs, albeit with moderate overpotentials, particularly in acid.[1,16] We note, however, that the on-electrode structure of most Cu-based catalysts is not known.[16]

Since Hc is stable in the presence of dioxygen and hydrogen peroxide, models for Hc might be more stable toward oxidative degradation in the high potential, aqueous, electrochemical
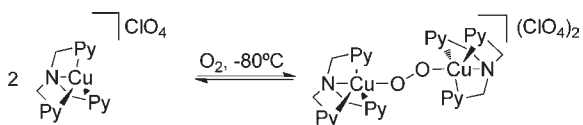
Figure 2. Illustration of [3]ClO$_4$ and the coordination of O$_2$ at low temperature.[20]

Figure 3. RRDE of **1** (red), **2** (blue), and XC-72 carbon black (black) with ring currents (dotted) in Britton—Robinson buffer under 1 atm of O$_2$ at 1600 rpm at pH 2 (a) and pH 10 (b).

environment, a requirement for practical ORR.[17,18] Hemocyanin also catalyzes the disproportionation of H$_2$O$_2$ to oxygen and water at neutral pH.[19] Inspired by these findings, we here investigate the ORR activity of Kodera's thermally stable hemocyanin model [Cu$_2$(bistripic)(NCMe)$_2$](PF$_6$)$_2$ (**2**) as well as the analogous monocopper complex [Cu(tripic)(NCMe)]PF$_6$ (**1**) (Figure 1). The monocopper complex **1** exhibits low affinity for dioxygen; the two tripicolinyl ligands must be tethered to observe O$_2$ coordination at room temperature.[15]

In contrast to the Hc model **2**, [CuTPA]$^+$ [TPA = tris(2-pyridylmethyl)amine] complexes react with dioxygen to form an end-on $\mu-\eta^1{:}\eta^1$-peroxo complex.[20,21] Although the O$_2$ adducts are only stable at low temperatures (−80 °C) (Figure 2), it is possible that this binding mode would be maintained on the electrode surface during ORR. Indeed, Karlin and co-workers evaluated [CuTPA]$^+$ in a nonaqueous environment for its ORR reactivity.[22] However, the behavior of [CuTPA]$^+$ in aqueous solution, supported on an electrode, is unknown. We thus examine the catalytic properties of the Cu^{II} analogue [CuTPA]-(ClO$_4$)$_2$, [3](ClO$_4$)$_2$.

■ EXPERIMENTAL SECTION

Catalyst Ink Preparation. Compounds **1** and **2** were synthesized as previously reported.[14,15,23] ^{1}H NMR spectra of both compounds matched the literature values. Carbon-supported catalysts **1** and **2** were prepared using Vulcan XC-72 (Cabot Corp.) carbon black in acetonitrile. First, 18 mg of carbon was sonicated for 15 min to ensure maximum dispersion. To this suspension was added 2 mg of the catalyst as a solid. The suspension was allowed to stand for 1 h, after which solvent was evaporated under a stream of air. To prepare an ink of the supported catalyst, the supported catalyst was sonicated in water (1 mg/mL) in the presence of 5 μL of a 5 wt % solution of Nafion (Sigma-Aldrich) per 1 mL of water. A 20 μL droplet of the ink was then evaporated onto a glassy carbon electrode (A = 0.196 cm^2) under a stream of Ar. By elemental analysis, Cu loadings were determined to be 8.8 mg/g of supported catalyst for compound **1** and 9.2 mg/g of supported catalyst for compound **2**. Control experiments utilized Vulcan XC-72 prepared identically but without compounds **1** or **2**.

Supported catalyst **3** was generated in situ by using TPA synthesized as previously reported.[24] A solution of [Cu(TPA)](ClO$_4$)$_2$ was prepared from 33.3 mg of Cu(ClO$_4$)$_2$·6H$_2$O (0.09 mmol, 99.999%, Alfa Aesar) and a solution of 26.1 mg (0.09 mmol) of TPA in 15 mL of ethanol. To this solution were added Vulcan XC-72 carbon black (54 mg) and 60 μL of a 5 wt % solution of Nafion (Sigma-Aldrich). The mixture was then sonicated for 30 min to disperse the carbon. The ink (10 μL) was then deposited directly onto the glassy carbon electrode and dried in air. Cu loading was found to be 5.56 mg/g of supported catalyst.

Reagents. Electrochemical experiments at pH 2−10 were performed in Britton—Robinson buffers consisting of 0.04 M CH$_3$CO$_2$H (99.99%, Sigma-Aldrich), 0.04 M H$_3$PO$_4$ (85 wt % in H$_2$O, 99.99%, Sigma-Aldrich), 0.04 M H$_3$BO$_3$ (99.999%, Sigma-Aldrich), and 0.1 M NaClO$_4$ (99.9%, Sigma-Aldrich) with Milli-Q water. Experiments performed at pH 1 were done in a solution of 0.1 M HClO$_4$ (70% Optima grade, Fisher Scientific). Hydrogen peroxide solutions (10 mM)
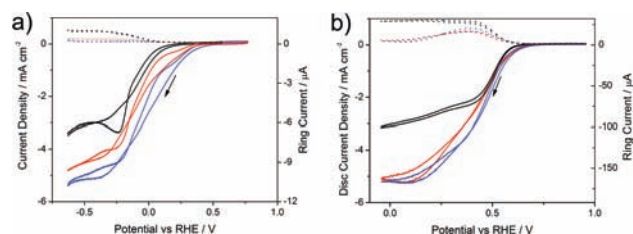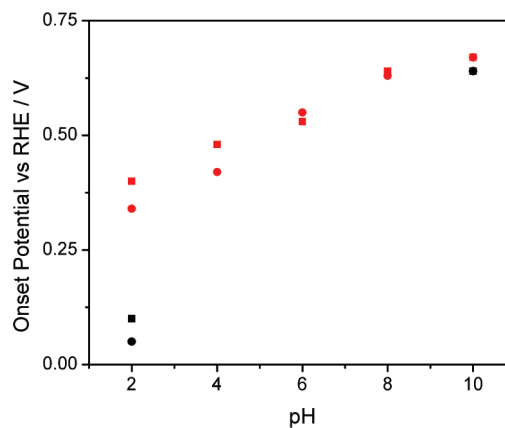

Figure 4. pH dependence of the onset potentials for O$_2$ (red) and H$_2$O$_2$ (black) reduction for **1** (circles) and **2** (squares). At pH 10, the onset potentials for both **1** and **2** overlap.

were made with 30 wt % H$_2$O$_2$ in water (30 wt % in H$_2$O, Ultrex II Ultrapure, Baker).

Electrochemical Experiments. Rotating disk electrode (RDE) and rotating ring—disk electrode (RRDE) electrochemical experiments were performed by using a glassy carbon working electrode (A = 0.196 cm^2) with a Pt ring (A = 0.093 cm^2, Pine Instruments), a Pt mesh counter electrode separated by a glass frit, and a Ag/AgCl "no-leak" (ESA, Inc.) reference electrode separated from the working electrode by a Luggin capillary. The Pt ring was held at 1.2 V vs reversible hydrogen electrode (RHE) for all experiments and the collection efficiency was determined to be 0.04 by comparison of the disk to ring currents for the 2e$^-$ reduction of O$_2$ to H$_2$O$_2$ for the unmodified Vulcan carbon.[25] The scan rate for all experiments was 5 mV/s, and all scans were performed starting with the cathodic sweep. All experiments were performed using a CH Instruments 760C bipotentiostat and a Pine Instruments MSRX rotator. All potentials reported were referenced to the RHE by flushing the cell with 1 atm of H$_2$ and measuring the open circuit potential at the Pt ring after experiments were completed.

■ RESULTS

Studies on Trispicolinylmethane Complexes. Initial studies focused on catalysis by compounds **1** and **2**, which were impregnated in inks composed of carbon black and Nafion. The results of RRDE voltammetry for these cathodes are presented in Figure 3 together with a control electrode lacking the copper complexes. When O$_2$ was excluded from the solution, voltammetry exhibited little current response from 0.75 V to at least −0.5 V. Following the introduction of O$_2$, however, a cathodic current was observed, the onset potential of which was

Table 1. Number of Electrons Transferred Determined from Koutecky−Levich Plots for 1, 2, and Vulcan Carbon in the Presence of O_2 or H_2O_2 at pH 2 and 10

	n_{O_2}		$n_{H_2O_2}$	
	pH 2 (−0.5 V)	pH 10 (0.07 V)	pH 2 (−0.5 V)	pH 10 (−0.5 V)
1	2.6	3.5	0.1	1.5
2	2.9	3.7	0.1	1.7
carbon black	2.8	2.3	0.8	0.8

Figure 6. Tafel plots of **1** (red), **2** (blue), and XC-72 Vulcan carbon black (black) in pH 2 (a) and pH 10 (b) Britton−Robinson buffer with 10 mM H_2O_2 under 1 atm of Ar with linear fits (dotted lines).
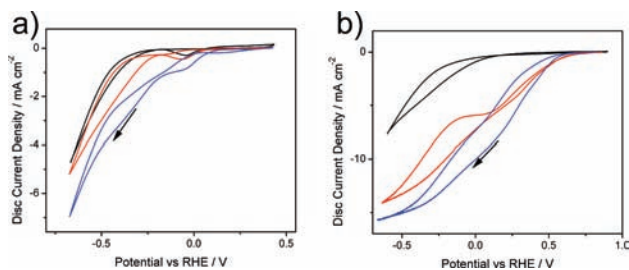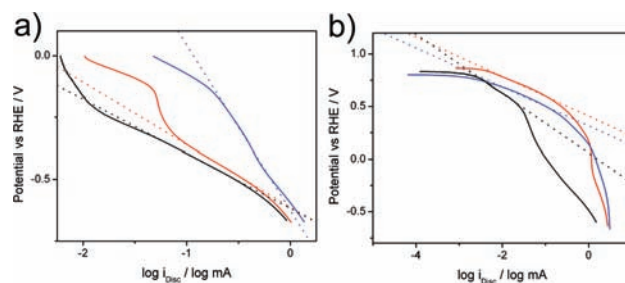

Figure 5. RDE of **1** (red), **2** (blue), and XC-72 carbon black (black) in Britton−Robinson buffer with 10 mM H_2O_2 under 1 atm of Ar at 1600 rpm at pH 2 (a) and pH 10 (b).

Figure 7. RRDE of [**3**](ClO_4)$_2$ in 0.1 M $HClO_4$ at pH 1 (a) and in pH 10 Britton−Robinson buffer (b) with ring currents (dotted lines) under 1 atm of Ar at 1600 rpm (black) and under 1 atm of O_2 at 1600 rpm (red), 800 rpm (blue), 400 rpm (green), and 200 rpm (orange).

found to depend on pH (Figure 4). At pH 2, the onset of oxygen reduction by compounds **2** and **1** was found at 0.40 and 0.34 V, respectively, whereas for the Vulcan carbon control, the onset was only 0.11 V. The limiting current for compound **2** is the largest at 5 mA cm^{-2}, that of **1** is slightly less at 4.5 mA cm^{-2}, and that of carbon black is the least at 3 mA cm^{-2}.

Shown in Table 1 is the number of electrons transferred by each catalyst, determined by a Koutecky−Levich plot made by varying the electrode rotation rate (Supporting Information). At pH 2, catalysts **1** and **2** as well as Vulcan carbon were found to transfer approximately 2e$^-$, consistent with reduction of O_2 to H_2O_2. In Figure 3, the positive currents arise from the Pt ring, held at 1.2 V to oxidize any produced peroxide. Whereas carbon black has the largest ring current, the number of electrons transferred by each catalyst, shown in Table 1, is similar.

At pH 10, the onset of O_2 reduction for **1** and **2** is more positive than at pH 2. The onset for **1** and **2** is 0.67 V, whereas the onset for carbon is at 0.60 V. The limiting currents for **1** and **2** are 5 mA cm^{-2}, whereas for carbon the current was 3 mA cm^{-2}. Although the current densities at pH 10 and 2 are similar, the number of electrons transferred at pH 10 is larger than at pH 2. The ring current in Figure 3b is also larger than in Figure 3a, corresponding to increased production of H_2O_2. The increase in the number of electrons transferred at pH 10 relative to pH 2 for both compounds along with the increase in ring current associated with peroxide oxidation seems initially contradictory (see Discussion).

Figure 5 shows RDE voltammograms of compounds **1**, **2**, and Vulcan carbon in Britton−Robinson buffer 10 mM H_2O_2 under 1 atm of Ar at pH 2 and 10. At pH 2, shown in Figure 3a, H_2O_2 reduction onset occurs at 0.05 V for compound **1**, 0.1 V for compound **2**, and 0.0 V for Vulcan carbon. The number of electrons transferred for all three compounds, determined from the Koutecky−Levich analysis, is far less than the 2e$^-$ value expected for peroxide reduction to water (Table 1). At pH 10,
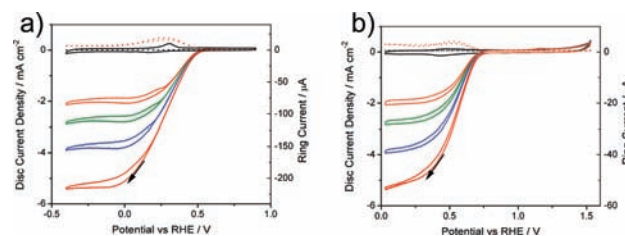
however, the catalytic activity of **1** and **2** for the reduction of H_2O_2 is improved, as shown by the increase of the onset potentials to 0.65 V for **1** and 0.64 V for **2** and an increase in the current densities (Figure 5b). Correspondingly at high pH, the number of electrons transferred approaches the 2e$^-$ value.

Tafel plots for all three catalysts at pH 2 and 10 with 10 mM H_2O_2 are presented in Figure 6. At pH 2, compounds **1** and **2** exhibit linear regions in their Tafel plots with slopes of −167 and −656 mV/decade, respectively (see Discussion). At pH 10, compounds **1** and **2** have similar slopes of approximately −187 mV/decade, whereas carbon black exhibits a much larger slope of −283 mV/decade. Tafel plots for dioxygen reduction at pH 2 and 10 can be found in the Supporting Information.

Studies on Trispyridylmethylamine Complexes. RRDE voltammetry results for catalysts prepared from [**3**](ClO_4)$_2$ in 0.1 M $HClO_4$ are shown in Figure 7a. At pH 1 under Ar, little current is observed, with the exception of a reversible couple at 0.23 V, which we assign to the Cu$^{I/II}$ couple.[26] With the addition of O_2, an increase in the cathodic current is noted, which is associated with the ORR. The onset of the reduction current is 0.53 V vs RHE. The ring current reveals that at potentials between the onset and the diffusion-limited current, hydrogen peroxide is formed. The diffusion-limited current changes with the rotation rate, which, after fitting to the Koutecky−Levich equation, shows that 3.8e$^-$ were transferred in the reduction.

The voltammetry of [**3**](ClO_4)$_2$ is similar at pH 1 and 10 (Figure 7). Under Ar, the Cu$^{I/II}$ couple is at 0.49 V at pH 10, which corresponds to a shift of 30 mV/pH unit. The onset of O_2 reduction at pH 10 is at 0.77 V, 240 mV more positive than at pH 1. The ring current once again shows that H_2O_2 is formed at potentials between the onset and the diffusion-limited current. Koutecky−Levich analysis of the dependence of the rotation rate on the reduction current also shows that 3.9e$^-$ were transferred at this pH.
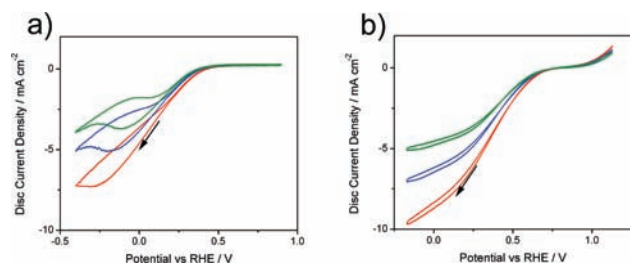
6160

dx.doi.org/10.1021/ic200386d |*Inorg. Chem.* 2011, 50, 6158−6162

Figure 8. RDE of $[3](ClO_4)_2$ in 0.1 M $HClO_4$ at pH 1 (a) and at pH 10 in Britton−Robinson buffer (b) with 10 mM H_2O_2 at 800 rpm (red), 400 rpm (blue), and 200 rpm (green).
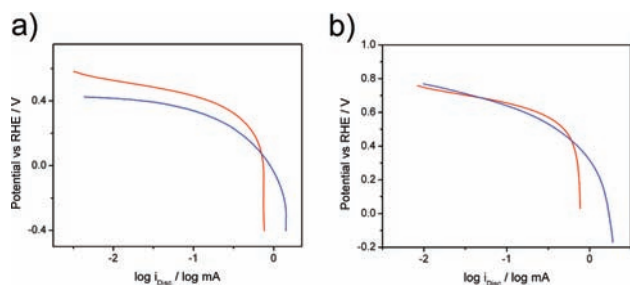

Figure 9. Tafel plots of $[3](ClO_4)_2$ in 0.1 M $HClO_4$ at pH 1 (a) and in pH 10 Britton−Robinson buffer (b) under 1 atm of O_2 (red line) and under 1 atm of Ar with 10 mM H_2O_2 (blue line).

The RDE voltammograms of $[3](ClO_4)_2$ under 1 atm of Ar with 10 mM H_2O_2 are shown in Figure 8. At pH 1, the onset of peroxide reduction is at 0.52 V, which is also the onset potential for dioxygen reduction. At pH 10, the onset is more positive at 0.73 V. The onset potentials for peroxide reduction seem to follow the onset potential of O_2 reduction (Figure 10). The number of electrons transferred is 2.0 at all pHs, consistent with reduction of H_2O_2 to H_2O.

Tafel plots of $[3](ClO_4)_2$ under 1 atm of O_2 and 1 atm Ar with 10 mM H_2O_2 are shown in Figure 9. The slopes of the linear regions at both pH 1 and 10 with O_2 or H_2O_2 are ∼70 mV/ decade. The pH dependence of the onset potential of O_2 reduction has two linear regions, as seen in Figure 10. At low pH, the onset potential changes from 0.53 V by 5 mV/pH unit. Above pH 4, the onset varies by 35 mV/pH, consistent with what has been observed for other copper complexes.[16,27] The change in slope is likely related to the pK_a of the TPA.[28] H_2O_2 reduction follows the same trend.

DISCUSSION

The most interesting information obtained from the comparison of complexes **1** and **2** relates to the different Tafel slopes and onset potentials, particularly at low pH. The relatively high Tafel slope for the dicopper complex **2** is consistent with a CE (chemical−electrochemical) mechanism for reduction.[29] Alternatively, the low slope for monomeric complex **1** is consistent with a simple electron transfer in the rate-determining step, an E mechanism.[30] The number of electrons transferred for **1** and **2** are both around 3, suggesting a 2e⁻ reduction of oxygen to peroxide, followed by slow (incomplete) 2e⁻ reduction of the formed H_2O_2 to water. The low activity for **1** and **2** is also seen in the low number of electrons transferred in H_2O_2 reduction at pH 2. Intriguingly, the
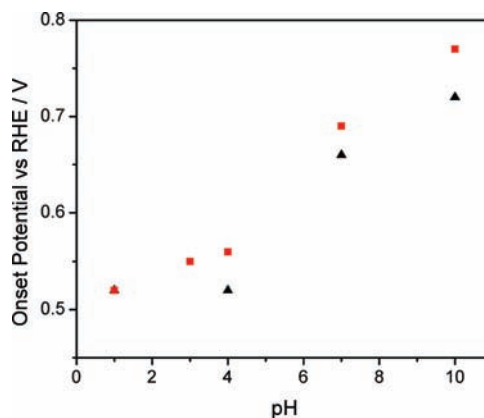

Figure 10. Plot of the pH dependence of the onset of O_2 reduction (red squares) and H_2O_2 reduction (black triangles) for $[3](ClO_4)_2$.

ORR onset potential for the dicopper complex is somewhat more positive than that found for the corresponding monomer.

At high pHs, **1** and **2** behave similarly in their ability to catalyze reduction of dioxygen and peroxide. These similarities apply to both onset potentials and Tafel slopes. The parallel behavior of **1** and **2** at high pH suggests a possible role of a cupric hydroxide intermediate that reacts with hydrogen peroxide to form the di-μ-peroxo complex. Kodera observed that $[Cu_2(OH)_2$-hexapy$]$ reacts with hydrogen peroxide to form the μ-peroxo complex.[31] We hypothesize that the Cu−OH species enhances the reaction rate of **1** and **2** with H_2O_2, increasing the apparent number of electrons transferred at high pH.

Compared to compounds **1** and **2**, the overpotentials for ORR exhibited by $[3](ClO_4)_2$ are lower by nearly 130 mV at low pH and 100 mV at pH 10. Remarkably, *the onset potential for ORR at pH 1 is the highest reported for any Cu complex.*[16,27,32−36] Additionally, the onset potential vs pH curve exhibits two linear regions, one between pH 1 and pH 4 and then another between pH 4 and pH 10. Also compound $[3](ClO_4)_2$ has an ORR Tafel slope considerably lower than those reported for any Cu complex.

We now address possible origins of the differences between compounds **1** and **2** and compound $[3]^{2+}$. First, we suggest that in the presence of O_2, $[3]^+$ dimerizes on the electrode surface. Evidence for dimerization comes from dilution measurements (Supporting Information) that show that ORR activity shifts to more negative potentials as the concentration of compound $[3](ClO_4)_2$ is lowered below ca. 0.001 mol %. Additionally, the ORR current does not scale linearly with catalyst loading over 2 orders of magnitude. The remarkably low Tafel slopes (ca. 70 mV/decade) are close to those expected for a two-electron transfer rate-limiting step (60 mV/decade), also suggesting that two Cu centers are involved.[29] In recent work, Karlin and co-workers reported the use of $[3](ClO_4)_2$ as a catalyst for the 4e⁻ reduction of O_2 in acetone.[22] The electron stoichiometry was analyzed using decamethylferrocene ($FeCp^*_2$) as an electron donor. Unfortunately, the high reactivity of $FeCp^*_2$ by itself toward O_2 in the presence of acid makes further evaluation of this system complicated.[37]

We propose that the differing catalytic properties of $[3]^{2+}$ vs **1** and **2** is related to the mode of O_2 coordination. In **2**, O_2 binds in a side-on peroxo, $\mu-\eta^2:\eta^2$ mode. However, $[3]^+$ binds O_2 to form an end-on, *trans*-$\mu-\eta^1:\eta^1$-peroxo complex, which is stable at low temperatures. The end-on Cu−O_2 binding mode is

nucleophilic and the peroxo ligand is easily protonated.[38] The side-on $\mu-\eta^2:\eta^2$-O_2 ligand is generally electrophilic and would be expected to be more easily reduced, not protonated.[39] Attempts to protonate the $2-O_2$ adduct with HBF_4 in CH_2Cl_2 gave no reaction (see Supporting Information). We propose that addition of an electron to the O_2^{2-} peroxo intermediate seen for **2** is likely the rate-limiting step, leading to a greater overpotential for the ORR.

Compounds **1** and **2** have low activity for the ORR based on the onset of reduction current. Chidsey et al. reported a $Cu^{II}-$ (2,9-diethylphenanthroline) complex that has on onset potential of 0.305 V vs NHE (0.58 V vs RHE, at pH 4.8).[35] Bilewicz reported ORR onset of 0.67 V vs RHE for a dicopper—hexaazamacrocycle (pH 7).[36] Finally, we found that $Cu^{II}-$ 3,5-diamino-1,2,4-triazole (CuDAT) has an onset of 0.73 V vs RHE at pH 7 and the highest reported onset of 0.86 V vs RHE at pH 13.[1,16] Compounds **1** and **2** are comparable to the Bilewicz work, and similarly, they follow a $2e^- + 2e^-$ mechanism.

Compound $[3](ClO_4)_2$ shows reduced ORR overpotentials compared to many compounds. At pH 1, $[3](ClO_4)_2$ has a 60 mV higher oxygen reduction onset than CuDAT. At pH 5, its onset is lower than that of $Cu^{II}-$(2,9-diethylphenanthroline) by 40 mV. At high pH, ORR by $[3](ClO_4)_2$ has an onset lower than that of CuDAT by 70 mV. The origin of this increased activity might be associated with optimized O_2 coordination by **3**.

■ CONCLUSION

A copper catalyst prepared from trispyridylmethylamine (TPA) exhibits a lower overpotential and higher activity for ORR than related complexes based on trispyridylmethane ligands. Relative to other complexes, catalysts based on TPA exhibit the highest reported onset potentials at pH 1 (0.53 V vs RHE). The differing catalytic behaviors are attributed to the differences in the modes by which these complexes interact with O_2, end-on vs side-on O_2 binding. These results encourage further efforts aimed at the development of new molecular electrocatalysts.

■ ASSOCIATED CONTENT

⑤ Supporting Information. Additional information as discussed in the text. This material is available free of charge via the Internet at http://pubs.acs.org.

■ AUTHOR INFORMATION

Corresponding Author
*Tel: 217-333-8329. Fax: 217-244-3186. E-mail: agewirth@ illinois.edu.

■ ACKNOWLEDGMENT

■ REFERENCES

(1) Gewirth, A. A.; Thorum, M. S. *Inorg. Chem.* **2010**, *49*, 3557.
(2) Chalk, S. G.; Miller, J. F.; Wagner, F. W. *J. Power Sources* **2000**, *86*, 40.
(3) Gasteiger, H. A.; Kocha, S. S.; Sompalli, B.; Wagner, F. T. *Appl. Catal., B* **2005**, *56*, 9.
(4) Gasteiger, H. A.; Panels, J. E.; Yan, S. G. *J. Power Sources* **2004**, *127*, 162.
(5) Marcinkoski, J.; Kopasz, J. P.; Benjamin, T. G. *Int. J. Hydrogen Energy* **2008**, *33*, 3894.
(6) Mano, N.; Soukharev, V.; Heller, A. *J. Phys. Chem. B* **2006**, *110*, 11180.
(7) Claus, H. *Micron* **2004**, *35*, 93.
(8) Solomon, E. I.; Augustine, A. J.; Yoon, J. *Dalton Trans.* **2008**, 3921.
(9) Solomon, E. I.; Chen, P.; Metz, M.; Lee, S.-K.; Palmer, A. E. *Angew. Chem., Int. Ed.* **2001**, *40*, 4570.
(10) Yoon, J.; Fujii, S.; Solomon, E. I. *Proc. Natl. Acad. Sci. U. S. A.* **2009**, *106*, 6585.
(11) De, A.; Mandal, S.; Mukherjee, R. *J. Inorg. Biochem.* **2008**, *102*, 1170.
(12) Decker, H.; Schweikardt, T.; Tuczek, F. *Angew. Chem., Int. Ed.* **2006**, *45*, 4546.
(13) Kodera, M.; Kajita, Y.; Tachi, Y.; Katayama, K.; Kano, K.; Hirota, S.; Fujinami, S.; Suzuki, M. *Angew. Chem., Int. Ed.* **2004**, *43*, 334.
(14) Kodera, M.; Kano, K. *Bull. Chem. Soc. Jpn.* **2007**, *80*, 662.
(15) Kodera, M.; Katayama, K.; Tachi, Y.; Kano, K.; Hirota, S.; Fujinami, S.; Suzuki, M. *J. Am. Chem. Soc.* **1999**, *121*, 11006.
(16) Thorum, M. S.; Yadav, J.; Gewirth, A. A. *Angew. Chem., Int. Ed.* **2009**, *48*, 165.
(17) Suzuki, K.; Shimokawa, C.; Morioka, C.; Itoh, S. *Biochemistry* **2008**, *47*, 7108.
(18) Andrew, C. R.; McKillop, K. P.; Sykes, A. G. *Biochim. Biophys. Acta Protein Struct. Mol. Enzymol.* **1993**, *1163*, 17.
(19) Ghiretti, F. *Arch. Biochem. Biophys.* **1956**, *63*, 165.
(20) Jacobson, R. R.; Tyeklar, Z.; Farooq, A.; Karlin, K. D.; Liu, S.; Zubieta, J. *J. Am. Chem. Soc.* **1988**, *110*, 3690.
(21) Karlin, K. D.; Tolman, W. B.; Kaderli, S.; Zuberbuehler, A. D. *J. Mol. Catal. A: Chem.* **1997**, *117*, 215.
(22) Fukuzumi, S.; Kotani, H.; Lucas, H. R.; Doi, K.; Suenobu, T.; Peterson, R. L.; Karlin, K. D. *J. Am. Chem. Soc.* **2010**, *132*, 6874.
(23) Kodera, M.; Kajita, Y.; Tachi, Y.; Kano, K. *Inorg. Chem.* **2003**, *42*, 1193.
(24) Canary, J. W.; Wang, Y.; Roy, R., Jr.; *Inorg. Synth.* **2007**, 70.
(25) Paulus, U. A.; Schmidt, T. J.; Gasteiger, H. A.; Behm, R. J. *J. Electroanal. Chem.* **2001**, *495*, 134.
(26) Nagao, H.; Komeda, N.; Mukaida, M.; Suzuki, M.; Tanaka, K. *Inorg. Chem.* **1996**, *35*, 6809.
(27) Zhang, J.; Anson, F. C. *J. Electroanal. Chem.* **1992**, *341*, 323.
(28) Anderegg, G.; Wenk, F. *Helv. Chim. Acta* **1967**, *50*, 2330.
(29) *Modern Electrochemistry*; Bockris, J. O. R., Amulya, K. N., Gamboa-Aldeco, M., Eds.; Plenum: New York, 2000.
(30) Delahay, P. *Double Layer and Electrode Kinetics*; Interscience Puhlishers: New York, 1965.
(31) Kodera, M.; Shimakoshi, H.; Tachi, Y.; Katayama, K.; Kano, K. *Chem. Lett.* **1998**, 441.
(32) Lei, Y.; Anson, F. C. *Inorg. Chem.* **1995**, *34*, 1083.
(33) Lei, Y.; Anson, F. C. *Inorg. Chem.* **1994**, *33*, 5003.
(34) Zhang, J.; Anson, F. C. *Electrochim. Acta* **1993**, *38*, 2423.
(35) McCrory, C. L.; Ottenwaelder, X.; Stack, T. D. P.; Christopher, C. E. D. *J. Phys. Chem. A* **2007**, *111*, 12641.
(36) Slowinski, K.; Kublik, Z.; Bilewicz, R.; Pietraszkiewicz, M. *J. Chem. Soc.—Chem. Commun.* **1994**, 1087.
(37) Su, B.; Nia, R. P.; Li, F.; Hojeij, M.; Prudent, M.; Corminboeuf, C.; Samec, Z.; Girault, H. H. *Angew. Chem., Int. Ed.* **2008**, *47*, 4675.
(38) Q. Hatcher, L.; D. Karlin, K. D. In *Advances in Inorganic Chemistry*; van Eldik, R., Reedijk, J., Eds.; Academic Press: New York, 2006; Vol. 58, p 131.
(39) Lewis, E. A.; Tolman, W. B. *Chem. Rev.* **2004**, *104*, 1047.